DERIVATION OF DYNAMIC FUNCTION PARAMETERS BY AREA SCANNING TECHNIQUES

W.J. MacIntyre, S.R. Inkley, E. Roth
W.P. Drescher and Y. Ishii
Department of Medicine, Case Western Reserve University; University Hospitals
Cleveland, Ohio, USA

ABSTRACT

This paper describes a functional imaging method for the study of organ function or organ blood flow and its application to the evaluation of lung ventilation and perfusion with ^{133}Xe. The method is based on area scintigraphy with a scintillation camera, data being accumulated on a 1600-channel analyzer as a 40 x 40 element matrix, transferred to magnetic tape and finally processed by a computer. For the evaluation of lung ventilation, the static distribution of ^{133}Xe in the lungs after inhalation of oxygen-^{133}Xe mixture is recorded as a single matrix during a 20-second period of breath holding. For the evaluation of lung perfusion successive matrices are recorded every 2 - 4 seconds after intravenous injection of a saline solution of ^{133}Xe so that the washout of ^{133}Xe from the lungs may be followed as a function of time. Each element of the matrices is initially subjected to a nine-element smoothing routine. The distribution of ventilation is then derived from the matrix for the static distribution of ^{133}Xe after its administration by inhalation and the distribution of perfusion from the relative slopes of the curves of disappearance of ^{133}Xe from the various matrix elements after its administration by injection. The results are displayed as a 40 x 40 element matrix of normalized values or alternatively as an isometric projection of a three-dimensional model in which the x and y co-ordinates give the spatial reference and the z co-ordinate the relative ventilation or perfusion. Typical results obtained by the method are presented and its advantages over methods which evaluate total organ function discussed.

In conventional measurements of organ function or organ blood flow, external probes are placed so that their fields of view will encompass the entire organ. Following this placement, a single recording such as a heart dilution curve, a renogram, or a hepatogram, can be analyzed to reflect the total blood flow or function of that organ. Recently, various investigators have recognized the applicability of stationary detector devices, or scintillation cameras, to serve as multiprobe detectors. Thus, multiple heart dilution curves (1, 2), renograms (3, 4), and lung washout curves (5, 6) have been recorded simultaneously by these systems.

The present investigation demonstrates that a sufficient number of flow or function curves may be recorded so that a complete functional visualization of an organ can be described with a display similar to a scan of the distribution of radioactivity in that organ. In this application, each spatial segment of the organ will have assigned to it a clearance rate or slope reflecting the rate in which the material is cleared or washed out from that segment (7, 8).

In order to integrate visually the regional variations of clearance, a scan display of the organ is reassembled with the x and y co-ordinates representing a flat projection of the organ in space and the z co-ordinate representing the magnitude of the rate constant instead of the magnitude of the radioactivity deposited.

The methodology described above has been called functional scanning (9) or functional imaging (10) and exhibits two primary criteria.

1. The first requisite is that an integrated description of the entire organ must be obtained. This differs from the multiprobe technique in that the function of the whole organ should now be visualized by one representation, similar to a conventional scan display, and not dependent on correlating multiple curves with sites from which the curves are derived selected by a separate visualization.

2. Secondly, the variation between adjacent sites must reflect differences in organ function or blood flow. This means that the relative magnitude of each spatial segment must represent some accepted parameter such as a disappearance constant, clearance rate, or half-time that will reflect the actual flow or function of that specific organ, not merely the amount of radioactivity deposited there.

Methodology

The technique of measurement for functional scanning of the lung is shown in Fig.1. For ventilation studies, ^{133}Xenon is distributed in the lung by the subject breathing an oxygen-xenon mixture from a 13.5 liter Collins respirometer to which 10 millicuries of ^{133}Xenon has been added to 10 liters of gas. For perfusion studies, 3 millicuries of ^{133}Xenon dissolved in saline are injected into an antecubital vein.

The distribution of radioactivity in the lung is detected by a Nuclear Chicago Pho-Gamma II scintillation camera and accumulated by an RIDL 1600 channel analyzer as a 40 x 40 word matrix. The diameter of the collimator is 10.5 inches so that each element of the 40 x 40 matrix can be represented spatially as a square with sides approximately one quarter inch long.

For measurement of the static distribution of ^{133}Xenon in the lungs from ventilation, a single matrix is recorded during a 20 second period of breath-holding following breathing of the oxygen-xenon mixture from the spirometer.

For perfusion studies, multiple distributions are required so as to be able to measure the washout of ^{133}Xenon from the lung as a function of time. To accomplish this purpose, matrices of the distribution are collected every 2.4 seconds and transferred to an Ampex TM-7291 digital tape recorder for processing by an IBM 360/40 computer.

To begin analysis, a conventional curve of accumulation and washout of the ^{133}Xenon by the entire lung field is determined by summation of all the counts in each matrix and plotting the relationship of total matrix counts versus the time in which each matrix was collected. The series of matrices immediately following the plateau or peak is then selected for determination of the washout slope.

Each element of the 40 x 40 matrices is initially subjected to a nine element smoothing routine involving bounding and averaging of the original counts in the matrix elements (11). The logarithm of the counts collected at each element on each frame is then fit by the method of least squares so as to obtain the optimum value of the disappearance constant, λ.

Thus:

$$\lambda = \frac{\sum y_i t - \frac{I}{N}\left[\sum y_i \sum t\right]}{\sum t^2 - \frac{I}{N}\left[\sum t\right]^2} \qquad \ldots\ldots(1)$$

where y_i is the logarithm of the counts in each element of the matrix, t is the time at which the matrix was collected, and N is the number of matrices used for calculation of the slope. N will vary dependent upon the half time of washout but it has been found that eight matrices are usually sufficient for determinati of the constant with sufficient accuracy.

It is assumed that for each matrix element a function exists of the form:

$$y_a = y_o e^{-\lambda t} \qquad \text{.....(2)}$$

where y_o can be calculated by the expression:

$$y_o = \frac{I}{N} \sum_i y_i - \frac{\lambda}{N} \sum t \qquad \text{.....(3)}$$

The standard derivation of λ is calculated by the expression:

$$\text{S.D. of } \lambda = \left[\frac{\sum (y_a - y)^2}{\left[\sum t^2 - \frac{I}{N} \left(\sum t \right)^2 \right] \left[N-2 \right]} \right]^{1/2} \qquad \text{.....(4)}$$

Where $(y_a - y)$ measures the deviation between values of the theoretical clearance curve, y_a and the actual recorded value, y. The initial distribution of the perfusion is determined by solving for the value of y_o at each matrix element. This value represents the total amount of radioisotope supplied to each element before any loss by washout occurs.

The matrices of the disappearance slopes and of distribution values obtaine from either ventilation or perfusion are subjected to a nine element bounding and averaging programme previously described. Following this smoothing, the final values are displayed both as a 40 x 40 matrix of normalized values or as a three-dimensional representation wherein the magnitude of either the distributio accumulation or the disappearance slope is shown as an isometric deflection of t z axis while the x and y co-ordinates maintain the spatial identification of the subject (11, 12).

The method of depicting relative slopes of the disappearance constant in a three-dimensional model is illustrated in Fig.2. Two elements of the 1600 - word matrix are shown with the larger disappearance constant (faster washout) corresponding to a greater height on the z axis. Assigning proportional heights to each of the 1600 elements thus results in a solid figure descriptive of the relative disappearance of ^{133}Xenon from every area of the lung field.

Results

The static distribution of ^{133}Xenon in the lungs of a patient recorded in the upright position following a 20 second breath-hold of ^{133}Xenon-oxygen is shown by the matrix of Fig.2A. The counts collected in each element of the matrix have been normalized and divided into 20 levels. In this distribution the number "1" represents the highest level of activity and "20" represents the lowest.

A similar matrix is shown in Fig.3B for the normalized disappearance constant, λ, derived for each matrix element. The number "1" represents the largest disappearance constant (fastest washout) and "20" represents the smallest constant (slowest washout).

Three dimensional models drawn from these matrices are shown in Fig.4 for the ventilation distribution of ^{133}Xenon in the lung and in Fig.5 for the disappearance slopes. Four views of the same lung are shown in which the matrix is viewed from each of the four corners (11). The two upper figures are being viewed from apex to base and the two lower representations are being viewed from base to apex.

Discussion

It is possible to obtain completely satisfactory function curves from direct playback of either continuous recording of the camera output on analog tape (1), video tape (13) or successive frames of digital tape (3) without data processing. These techniques are applicable when either a limited number of sites are required, when the combination of counting rate and accumulation time will yield the desired statistical accuracy, or when qualitative viewing is sufficient.

When, as in most applications of functional scanning, a large number of elements are required so as to visualize an entire organ, or when it is necessary that the desired parameter be derived by some process such as least squares fitting, a computer of appreciable capabilities must be considered as an integral part of the functional scanning system.

The selection of the three-dimensional scan as a readout is not, necessarily, a requisite for the functional concept. Other types of readouts may well be used, provided several criteria are met.

1. The primary requisite is one of linearity. It is necessary that a wide range of values be visualized with equal perception, not merely that the presence of "hot" areas or "cold" areas be identified on a distribution scan. Accentuation techniques, such as photoscanning, are difficult therefore, to adapt to this condition.

2. Secondly, it is desirable to be able to ascertain small differences between values. Except in gross situations, function may not be expected to vary greatly between adjacent areas. Thus, it is important to be able to perceive small differences and to have the differences readily apparent to the eye. The numerical readout of the matrix is linear, but it is difficult to visualize readily small variations by reading numbers.

The resolution of the system will be dependent upon the collimator, the inherent resolution of the imaging device, and the smoothing function used in computer analysis. The approximate quarter inch dimensions of the matrix elements are considerably small than the resolution of the system. As with most display systems, however, we have found that sampling at several fold the rate of the maximum spatial frequency component improves the visual integration of the distribution.

A distribution of ^{133}Xenon in the lung following spirometer administration is shown in Fig.6 as analyzed by our original distributions as a 18 x 18 matrix (324 elements) and the identical orientation on the same patient five months later with our present 40 x 40 (1600 element) matrix. The visualization is improved even though the inherent resolution is the same in both studies.

In summary, it can be said that this technique of functional scanning has demonstrated that it is entirely practical to obtain a single display of the function of an organ in the same manner as the conventional distribution representations. Rather than the clinician being concerned with selection of specific regions and interpreting curves from selective sites, the entire organ function can now be displayed with the number of independent sites determined by the resolution of the system and on statistical limitations.

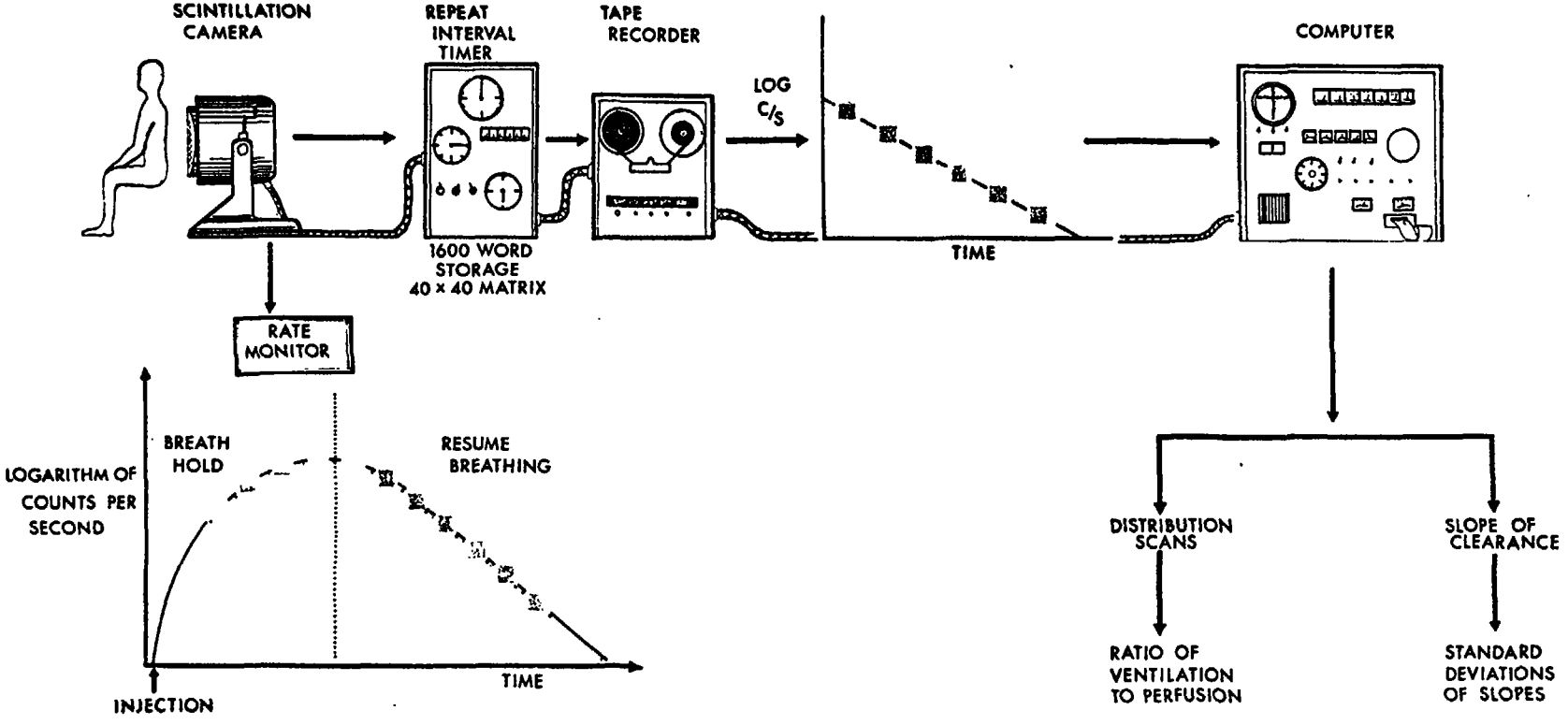

Fig.1. Scheme for recording time sequential distribution of regional radioisotope deposition for derivation of functional parameter displays.

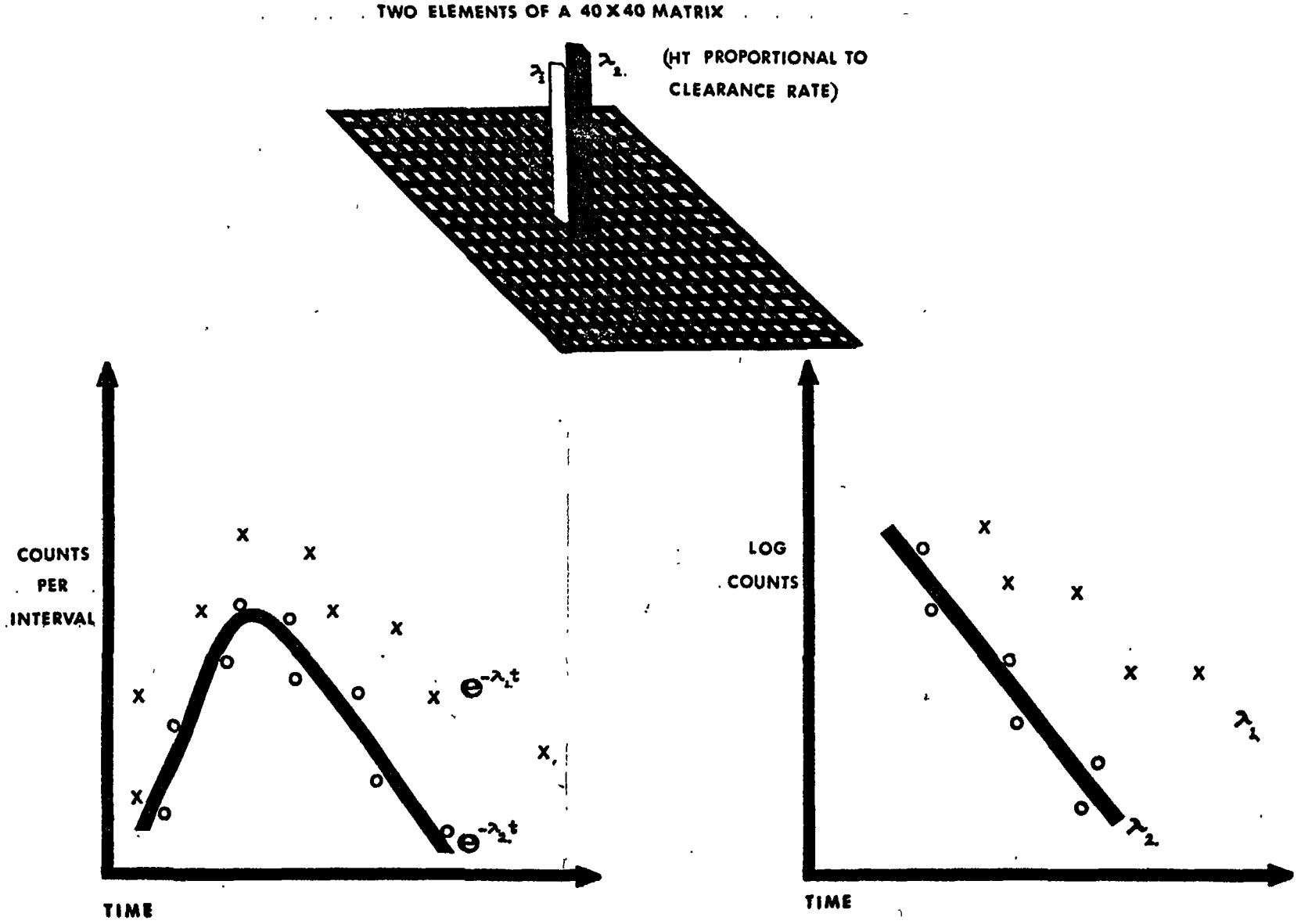

Fig.2. Technique for construction of three-dimensional model of slopes of the disappearance of 133Xenon from the lung. Two relative slopes are shown with height proportional to the rate of clearance.

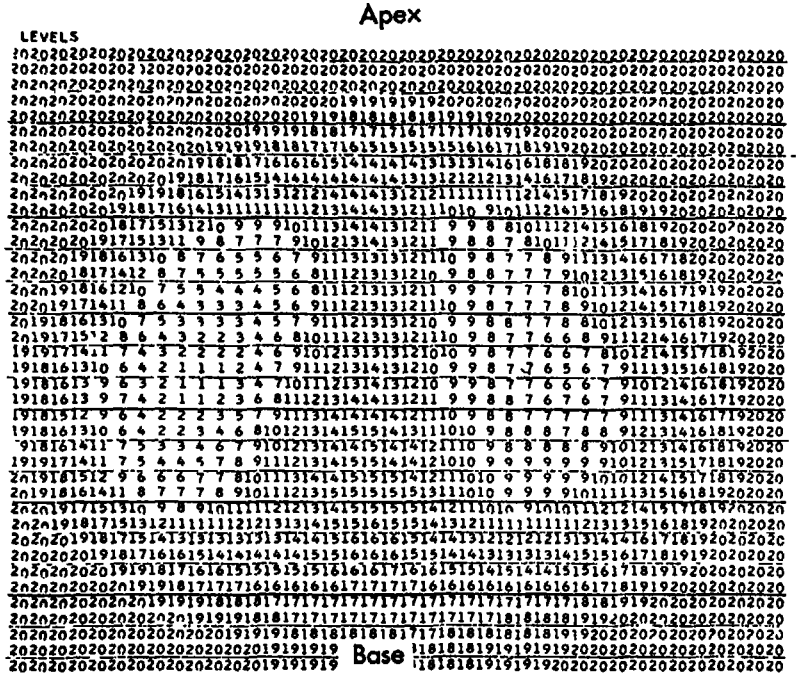

(A) Distribution in lung

Fig.3A. Matrix of relative magnitudes of ^{133}Xenon distribution in the lung following inhalation. The number "1" represents the highest quantity of activity and number "20" represents the lowest.

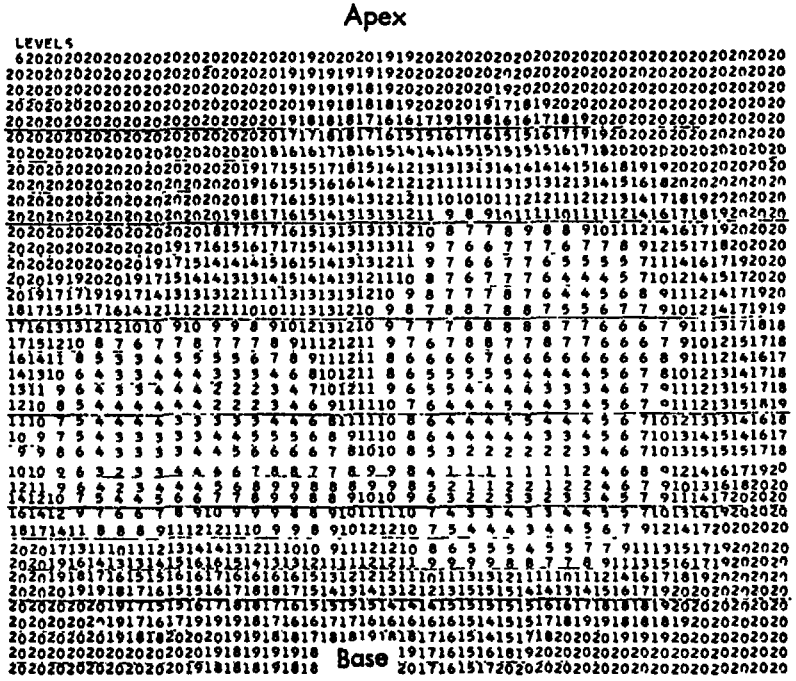

(B) Slopes of disappearance curves

Fig.3B. Matrix of relative magnitudes of the disappearance slopes of ^{133}Xenon washout from the lung following intravenous injection. Note decreased clearance rate in upper right lung field not predicted by the distribution levels in (A). The number "1" represents the fastest washout and "20" represents the slowest.

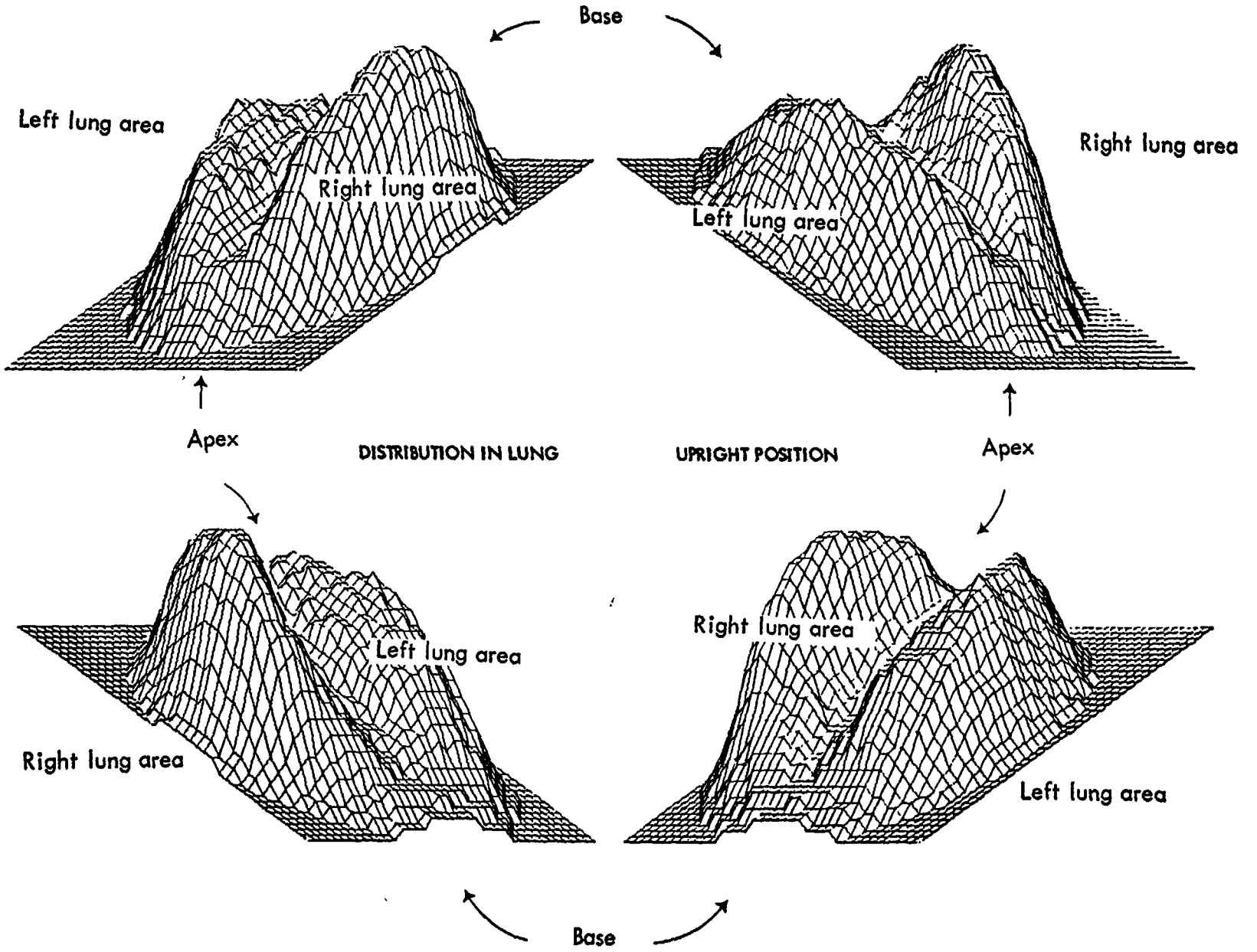

Fig.4. Three-dimensional view of matrix of Fig.3A showing ventilation distribution of ^{133}Xenon following inhalation. Four views of the same lung are shown, each viewing the matrix from one of the four corners.

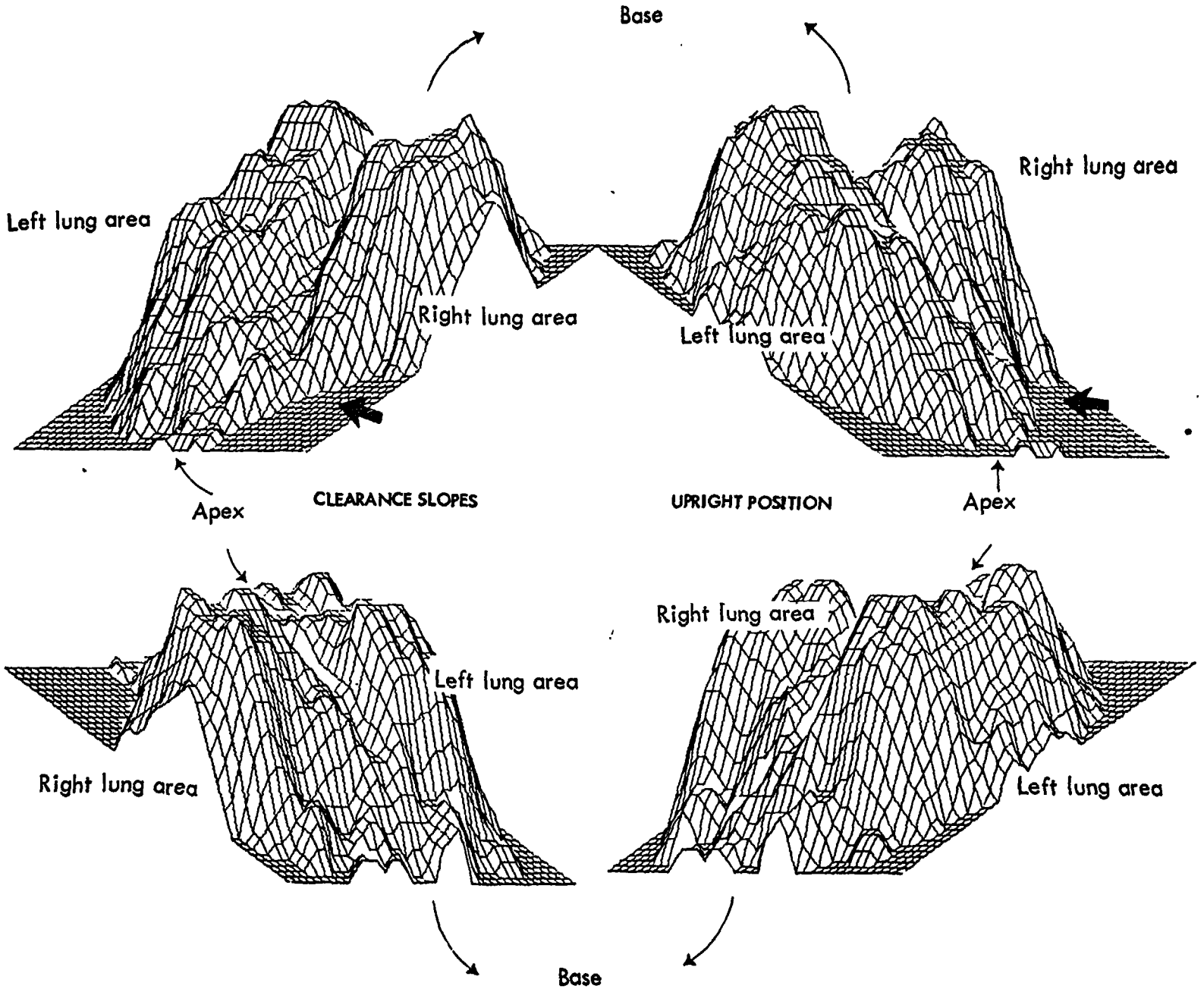

Fig.5. Three-dimensional view of matrix of Fig.3B showing relative magnitudes of the disappearance slopes following intravenous injection of ^{133}Xenon. Highest levels represent regions of most rapid disappearance of the Xenon. Heavy arrows mark the region of low clearance seen in matrix 3B which is due to absence of perfusion in this area since ventilation is normal as seen in Fig.3A.

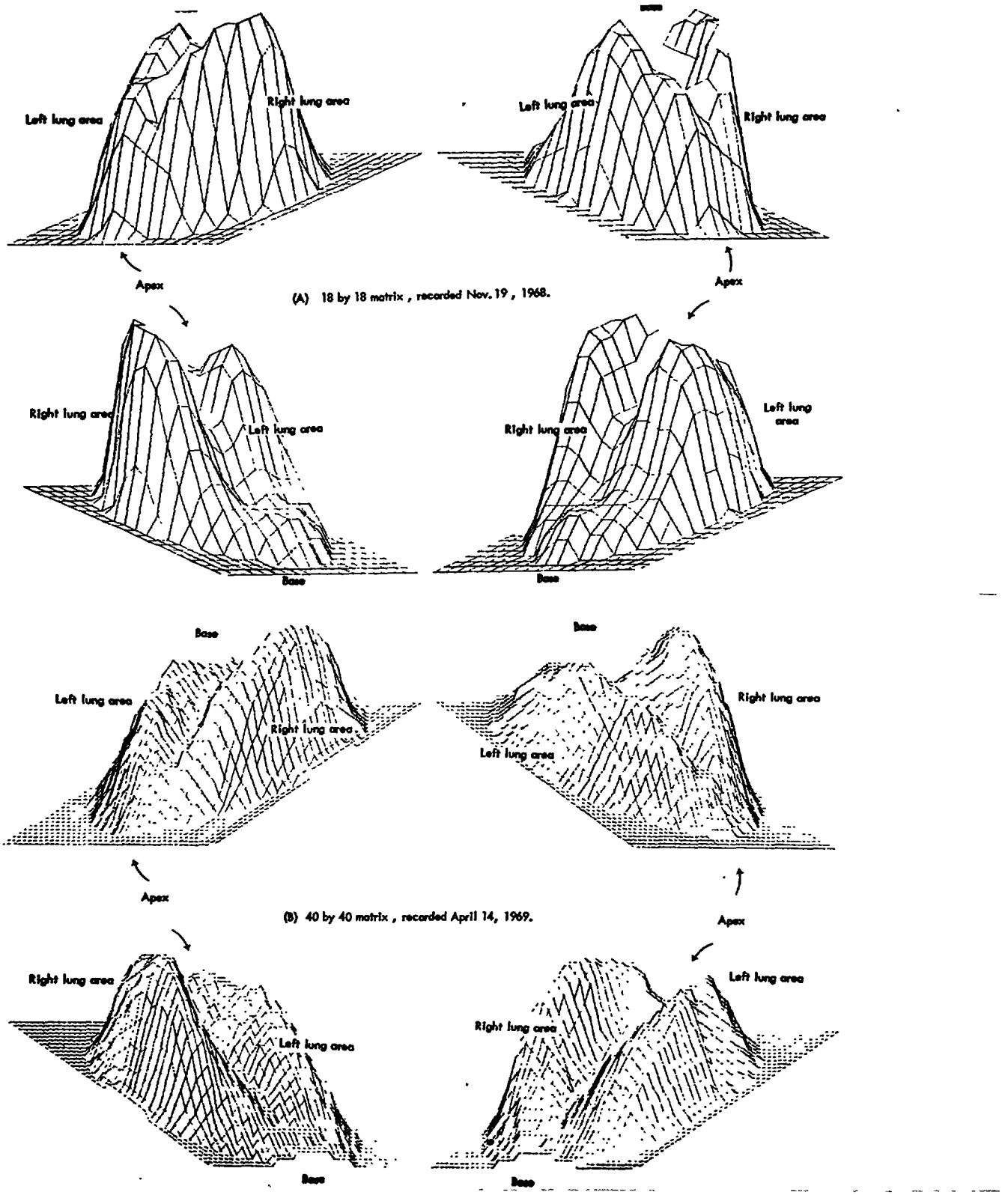

Fig.6. Effect of matrix size on visualization of regional variations. The upper display of 324 elements was recorded on November 19, 1968 on the patient shown in Fig.3 prior to a surgical procedure for bullous emphysema.

Lower figure was recorded 146 days after the upper display when matrix size had been expanded to 1600 elements.

REFERENCES

(1) ADAM, W.E., SCHENCK, P., KAMPMANN, H., LORENZ, W.J., SCHNEIDER, W.G., AMMANN, W., BILANIUK, L., Medical Radioisotope Scintigraphy 2, IAEA, Vienna (1969) 77.

(2) BENDER, M.A., MOUSSA-MAHMOUD, L., BLAU, M., Medical Radioisotope Scintigraphy 2, IAEA, Vienna (1969) 57.

(3) SIGMEN, E.M., BENDER, M.A., BLAU, M., J. Urol. (Baltimore) 92 (1964) 153.

(4) LOKEN, M.K., LINNEMANN, R.E., KUSH, G.S., Radiology 93 (1969) 85.

(5) MEDINA, J.R., LILLEHIE, J.P., LOKEN, M.K., EBERT, R.V., J. Amer. med. Ass. 208 (1969) 985.

(6) INKLEY, S.R., MACINTYRE, W.J., J. Lab. clin. Med. 74 (1969) 885.

(7) LOVE, W.D., PULLEY, P.E., Clin. Res. 14 (1966) 83.

(8) SMITH, R.O., LOVE, W.D., ISHARA, Y., ELLIOTT, M.S., LEHAN, P.H., J. nucl. Med. 9 (1968) 348.

(9) MACINTYRE, W.J., INKLEY, S.R., J. nucl. Med. 10 (1969) 355.

(10) KAIHARA, S., NATARAJAN, T.K., WAGNER, H.N., Jr., MAYNARD, C.D., J. nucl. Med. 10 (1969) 347.

(11) MACINTYRE, W.J., CHRISTIE, J.H., CURTIS, G.S., Radiology 90 (1968) 22.

(12) MACINTYRE, W.J., CHRISTIE, J.H., Medical Radioisotope Scintigraphy 1, IAEA, Vienna (1969) 771.

(13) ASHBURN, W.L., HARBERT, J.C., WHITEHOUSE, W.C., MASON, D.T., J. nucl. Med. 9 (1968) 554.